*Int. J. Electrochem. Sci.*, 14 **(2019)** 9206 – 9220, doi: 10.20964/2019.09.57

International Journal of
ELECTROCHEMICAL
SCIENCE
www.electrochemsci.org

# Carbohydrates as Corrosion Inhibitors of API 5L X70 Steel Immersed in Acid Medium

*Araceli Espinoza Vázquez*[1], *Manuel Alejandro Cervantes Robles*[2], *Guillermo E. Negrón Silva* [2,*], *Francisco Javier Rodríguez Gómez*[1], *Manuel Palomar Pardavé*[3], *Leticia Lomas Romero*[4], *Deyanira Ángeles Beltrán*[2], *Diego Pérez Martínez*[4]

[1] Universidad Nacional Autónoma de México, Departamento de Ingeniería Metalúrgica. Av. Universidad No. 3000, Delegación Coyoacán México. C.P. 04510. México.
[2] Universidad Autónoma Metropolitana, Departamento de Ciencias Básicas y Departamento de Materiales.
[3] Av. San Pablo No. 180, Azcapotzalco, Ciudad de México. C.P. 02200. México.
[4] Universidad Autónoma Metropolitana, Departamento de Química. Av. San Rafael Atlixco No.186, Iztapalapa, Cuidad de México. C.P. 09340. México.
[*]E-mail: gns@azc.uam.mx

*Received:* 9 March 2019 / *Accepted:* 10 July 2019 / *Published:* 5 August 2019

Commercially available carbohydrates D(+)-glucose (1), D(+)galactose (2) and lactose (3), along with some synthesized derivatives Methyl-4,6-O-Benzylidene-α-D-glucopyranosae (4), Methyl 4,6-O-benzylidene-2-O-p-toluenesulfonyl-α-D-glucopyranose (5), Methyl 4,6-O-benzylidene-2,3-di-O-p-toluenesulfonyl-α-D-glucopyranose (6), Methyl 2,3-anhydro-4,6-O-benzylidene-α-D-mannopyranose (7) and 6-methoxy-2-phenyl-7- (prop-2-yn-1-yloxy) hexahydropyran [3,2-d] [1,3] dioxin-8-ol (8), have been evaluated as corrosion inhibitors for API 5L X70 steel immersed in HCl 1M, with stationary conditions. The best corrosion inhibition was achieved by Methyl-4,6-O-Benzylidene-α-D-glucopyranose (4), with 87% efficiency at 50 ppm. Worth noting, D(+)-glucose (1) performed better as a corrosion inhibitor than D(+)galactose (2). Langmuir isotherm studies showed that all the compounds followed a combined chemical-physical adsorption process (according to the Gibbs energy data analysis). SEM-EDS studies confirmed the decrease of the corrosion process on the steel surface in the presence of the corrosion inhibitors.

**Keywords:** carbohydrates, API 5L X70, inhibitors.

## 1. INTRODUCTION

Corrosion of carbon steel in aqueous solution, which is an electrochemical process involving iron dissolution from steel and hydrogen evolving, has been widely recognized as one of the principal factors

of steel degradation in oil and gas pipelines [1-3]. To effectively solve this problem, several studies have been conducted using corrosion inhibitors [4], which are organic or inorganic chemical substances that effectively decrease the corrosion process on a metal surface when are added in low quantities to the corrosive medium [5]. In the search for environment-friendly corrosion inhibitors, organic compounds derived from carbohydrates, like chitosan [6] or aloe vera [7], have been tested with promising results.

Carbohydrates are the most abundant compounds in the biological world, which represents more than 50% of the total dry weight of earth biomass. Their functions include structural composition and recognition sites in cells, and as the main source of metabolic energy [8]. In this regard, D(+)-glucose (1) is the most abundant carbohydrate in nature (figure 1(**3**)). Living cells oxidize D(+)-glucose to obtain energy and to synthesize glycogen as energy reserve [9].

Taking in account that carbohydrates are low-cost and readily-available compounds and the relatively easiness to obtain carbohydrate derivatives, we proceeded to evaluate them as corrosion inhibitors of API 5L X70 steel under acidic conditions, by electrochemical impedance spectroscopy (EIS) test.

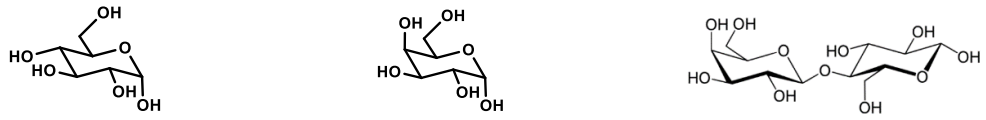


**Figure 1.** Chemical structure of the commercial carbohydrates D(+)-glucose (1), D(+)galactose (2) and lactose (3).

## 2. EXPERIMENTAL

### *2.1 Synthesis of the carbohydrate derivatives*

#### *2.1.1 Methoxy-4,6-O-Benzylidene-α-D-glucopyranose (4)*

The preparation of the compound 4 was made from the precursor's methyl-α-D-glucopyranose (1.2 equivalents), zinc chloride 15 g (0.75 equivalents) and Benzaldehyde 50 mL (590 mmol). The reaction was carried out in a 250 ml ball flask at room temperature for 48 hours of vigorous stirring, at the end of the reaction time it was slowly emptied into a vessel containing cold water in constant agitation for 15 minutes, after this time a white solid is formed which is left in refrigeration for 12 hours, then the solid is extracted by decantation and placed under stirring for 1 hour with 50 ml of petroleum ether to remove the excess of benzaldehyde, after this time the solid is filtered in a funnel of the porous filter and subjected to 2 washes with deionized water and subsequently to 2 washes with petroleum ether, the solid is allowed to dry at room temperature for 12 hours and subsequently dry by heating to 70 ºC and reduced pressure in vacuum line obtaining a white solid with a yield of 63% of the reaction m.p. 145-147 ºC.

*2.1.2 Methyl 4,6-O-benzylidene-2-O-p-toluenesulfonyl-α-D-glucopyranose (5)*

Compound 4 (1 equivalent) was dissolved in anhydrous pyridine, then 1.25 equivalents of p-toluenesulfonyl chloride was slowly added to the solution in an ice bath with vigorous stirring. The mixture was allowed to react for 72 hours and was followed by thin-layer chromatography. After this time, the mixture was extracted with $CH_2Cl_2$ three times in an extraction funnel, the first one with a 10% HCl solution followed by one with a saturated solution of $NH_4Cl$ and finally with a saturated solution of NaCl. Then, the mixture was dried using $Na_2SO_4$ subsequently filtered and dried under reduced pressure. Finally, the product was recrystallized using a mixture of $CH_2Cl_2$ / Petroleum ether to obtain a white solid. Yield 88%, crystals with a m.p. of 152-155 $^oC$.

*2.1.3 Methyl 4,6-O-benzylidene-2,3-di-O-p-toluenesulfonyl-α-D-glucopyranose (6)*

One equivalent of compound 5 was dissolved in anhydrous pyridine; then 2.5 equivalents of p-toluenesulfonyl chloride was slowly added to the mixture in an ice bath with vigorous stirring, the mixture was left to react for 72 hours and was followed by thin layer chromatography. After this time the mixture was extracted with $CH_2Cl_2$ three times in an extraction funnel, the first one with a 10% HCl solution followed by one with a saturated solution of $NH_4Cl$ and finally with a saturated solution of NaCl. Then, the mixture was dried using $Na_2SO_4$, subsequently filtered and dried under reduced pressure. Finally, the product was recrystallized using a mixture of $CH_2Cl_2$ / Petroleum ether obtaining a white solid. Yield 65%, crystals with a m.p. of 147-149 $^oC$.

*2.1.4 Methyl 2,3-anhydro-4,6-O-benzylidene-α-D-mannopyranose (7)*

0.7 equivalent methyl 4,6-O-benzylidene-2-O-p-toluenesulfonyl-α-D-glucopyranose were dissolved in $CH_2Cl_2$. Then, 1.5 equivalents of metallic sodium (previously dissolved in methanol) are added dropwise to the solution using an addition funnel. The reaction is left for 48 hours at room temperature with constant stirring. After this time, the organic phase is extracted with dichloromethane and washed with a solution of $NH_4Cl$ and NaCl using an extraction funnel. The solution was dried using anhydrous $Na_2SO_4$ and finally evaporated to dryness under reduced pressure obtaining a white solid with. Yield 40% and m.p of 145-147 $^oC$.

*2.1.5 6-methoxy-2-phenyl-7- (prop-2-yn-1-yloxy) hexahydropyran [3,2-d] [1,3] dioxin-8-ol (8)*

In order to obtain the monopropargylated derivative, 1 equivalent of methoxy-4,6-O-Benzylidene-D-glucopyranose was used, which is dissolved in DMF and reacted with 0.9 equivalents of propargyl Bromide and 0.9 equivalents of Sodium Hydride. The reaction is left for 24 hours. After this time, the organic phase is extracted with dichloromethane and washed with a solution of $NH_4Cl$ and NaCl using an extraction funnel. The solution is dried using anhydrous $Na_2SO_4$ Finally, the product was

purified by chromatographic column using a mixture of ethyl acetate / petroleum ether (33/67) to obtain a white solid. Yield 55%, crystals with a m.p. of 115-118 $^{o}$C.

### *2.2 Corrosion inhibition tests*

#### *2.2.1 Inhibitor solutions*

A 0.01 M solution of each of the carbohydrates 1–8 in water or DMF was prepared. Then, concentrations of 5, 10, 20 and 50 ppm of the inhibitor were added to the HCl 1M corrosive solution.

#### *2.2.2 Electrochemical evaluation*

The potential was stabilized at 20 °C for approximately 1800 s before electrochemical impedance spectroscopy (EIS) test. EIS: a sinusoidal potential of ±10 mV was applied in a frequency interval of $10^{-2}$ Hz to $10^{4}$ Hz, in an electrochemical cell with three electrodes using Gill Ac. The working electrode was API 5L X70 steel, while reference electrode and counter electrode were Ag/AgCl saturated with chloride potassium and graphite respectively. The electrode surface was prepared using conventional metallography methods over an exposed area of 1 cm$^2$.

After EIS measurements, the potentiodynamic polarization curves at 50 ppm inhibitors. The measurements covered a range of -500 mV to 500 mV regarding the open circuit potential (OCP), with a sweep velocity of 66.07 mV/min using the ACM Analysis software for data interpretation

#### *2.2.3. Characterization of surfaces by SEM-EDS*

API 5L X70 steel was used for the corrosion inhibition studies. This type of steel has a metallographic preparation with the following nominal composition (wt%): C, 0.26; Mn, 1.65; P, 0.030; S, 0.030; and balance iron. The API 5L X70 steel surface was prepared both with and without (blank) inhibitor; a 50-ppm concentration was used for a 24 hours immersion time. After that experiment, the steel was washed with distilled water, dried, and the surface analyzed using a Zeiss SUPRA 55 VP electronic sweep microscope at 10 kV with a 300x secondary electron detector.

## 3. RESULTS AND DISCUSSION

### *3.1 Corrosion inhibition test by EIS for commercially available carbohydrates for API 5L X70 steel in acid conditions.*

Nyquist diagram for API 5L X70 steel without inhibitor is shown in figure 2, where can be observed that $Z_{real}$ value reached a maximum 40 Ω cm$^2$.

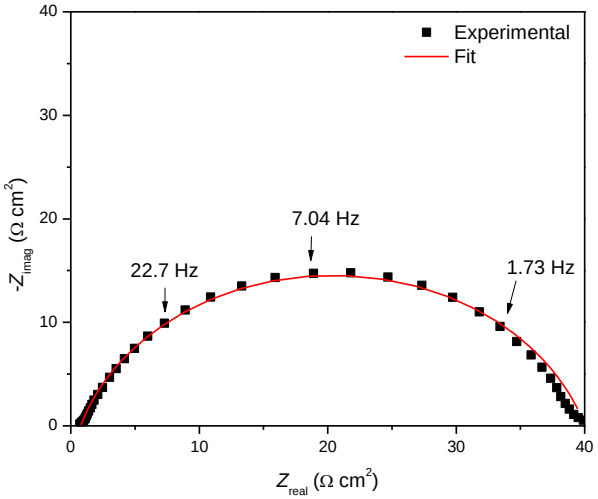


**Figure 2.** Nyquist diagram of API 5L X70 steel in HCl 1M

Nyquist diagrams for the systems with the corresponding commercially available carbohydrate inhibitors are shown in figure 3: D(+)-Glucose (3a), D(+)Galactose (3b) and Lactose (3c). These inhibitors showed a continuous increase in $Z_{real}$ value when increasing its concentration. The semi-circle shape of the diagrams it is an indicative of a time constant for D(+)-Glucose (4a) and D(+)Galactose (4b) controlled by charge transfer resistance [14]. However, Lactose (4c) showed a depressed curve, which is an indicative of the presence of two-time constants: one related to charge transfer resistance, and another one related to the adsorbed inhibitor film [10-12].

It is worth mentioning that both D(+)-Glucose and D(+)Galactose are structurally very similar, however, the position of the -OH could favor a larger semi-circle diameter in D(+)-Glucose Nyquist diagram. Lactose is a disaccharide formed by glucose and galactose moieties. The later could be the reason for a notable increment in semi-circle diameter ($Z_{real}$~ 325 Ω cm$^2$) at 50 ppm, and the glucose moiety could be responsible for the corrosion inhibition activity found in Lactose.

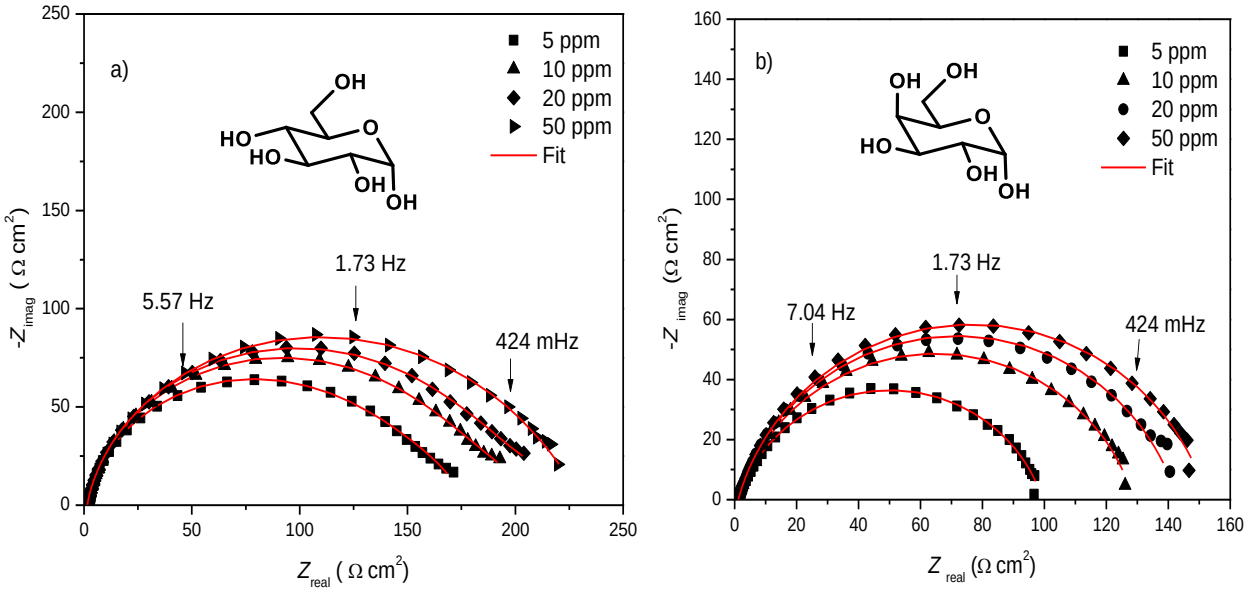

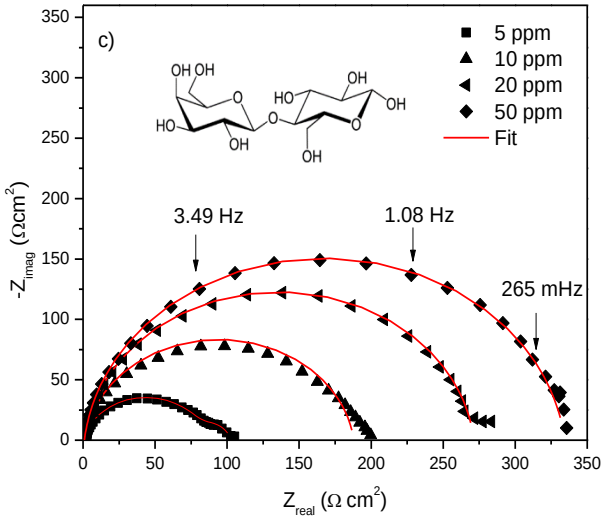


**Figure 3.** Nyquist diagrams of commercially available carbohydrate on immerse API 5L X70 steel at different inhibitor concentrations. Diagrams a), b), and c) corresponds to compounds D(+)-Glucose, D(+)Galactose and Lactose respectively.

After obtaining the Nyquist diagrams of the compounds at different concentrations (figure 3), the impedance results for API 5L X70 steel with and without inhibitor can be explained by an equivalent circuit (Figure 4) which comprise of $R_{ct}$ (charge transfer resistance), and $Q$ is the constant phase element in parallel with $R_s$ (solution resistance), $R_{mol}$ is the molecule resistance. Electrochemistry parameters are summarized in table 1.

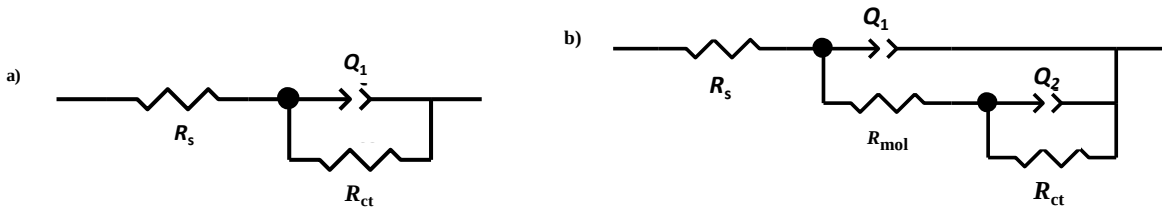


**Figure 4.** Equivalent electric circuit used in the system with (b) and without inhibitor (a).

Constant phase elements (CPE) have widely been used to account for deviations brought about by surface roughness. The impedance of CPE is given by the next equation [15]:

$$Z_{CPE} = Q^{-1}(j\omega)^{-n} \quad (1)$$

where $Q$ is the pseudo capacitance, $\omega$ is the angular frequency in rad $s^{-1}$, $j$ = -1 is the current density, and α is the CPE exponent. Depending on n, CPE may represent the resistance (Z (CPE) = r, n = 0), capacitance (Z (CPE) = C, n = 1), the inductance (Z (CPE) = L, n = -1) or the Warburg impedance for (n = 0.5). The CPE parameter $Q$ cannot represent the capacitance when n < 1 [16, 17].

$$C_{dl} = Y_0\left(\omega_m^{''}\right)^{n-1} \quad (2)$$

where $C_{dl}$ is the double layer capacitance and $\omega_m^{''}$ is the angular frequency in which $Z'$ is the maximum (Eq. 2).

The value of inhibition efficiency (*IE*) can be obtained by means of the following equation [13-14]:

$$\boldsymbol{IE}\ (\%) = \frac{\left(\frac{1}{\boldsymbol{Rct}}\right)\mathbf{blank} - \left(\frac{1}{\boldsymbol{Rct}}\right)\mathbf{inhibitor}}{\left(\frac{1}{\boldsymbol{Rct}}\right)\mathbf{blank}}\ \boldsymbol{x}\ \mathbf{100} \qquad \mathbf{(3)}$$

Where $R_{ct}$ is the charge transfer resistance with inhibitor and without inhibitor (blank).

As can be seen in table 1, the values of charge transfer resistance ($R_{ct}$) increase proportionally with an increment in inhibitor concentration. This can be attributed to a better protection of the metal Surface in the presence of the carbohydrates. Interestingly, glucose and galactose showed a similar performance as corrosion inhibitors, and, apparently, -OH orientation does not influence in the overall performance. However, Lactose showed the larger $R_{ct}$ values, which denotes a better API 5L X70 steel surface protection.

On the other hand, the decrease in the electrochemist double layer capacitance is generally associated to a displacement of solvent (water) molecules, which are replaced with inhibitor molecules, generating a protecting film [18-20].

**Table 1.** Electrochemical parameters of D(+)-Glucose, D(+)Galactose, and lactose in API 5L X70 steel immerse in HCl 1M

| **Inhibitor** | ***C*** **(ppm)** | $\boldsymbol{R_s}$ **(Ω cm²)** | **N** | $\boldsymbol{C_{dl}}$ **(μF cm⁻²)** | $\boldsymbol{R_{ct}}$ **(Ω cm²)** | $\boldsymbol{R_{mol}}$ **(Ω cm²)** | ***IE*** **(%)** |
|---|---|---|---|---|---|---|---|
| **Blank** | 0 | 5 | 0.8 | 1490 | 50 | - | - |
| **1** | 5 | 1.4 | 0.8 | 364.5 | 165.5 | - | 69.8 |
| | 10 | 1.4 | 0.8 | 385.5 | 191.8 | - | 73.9 |
| | 20 | 1.4 | 0.8 | 398.6 | 210.9 | - | 76.3 |
| | 50 | 1.4 | 0.8 | 439.3 | 226.4 | - | 77.9 |
| **2** | 5 | 0.9 | 0.8 | 796.3 | 98.5 | - | 60.1 |
| | 10 | 0.9 | 0.8 | 820.3 | 127.9 | - | 69.3 |
| | 20 | 1.2 | 0.8 | 863.5 | 141.9 | - | 72.3 |
| | 50 | 1.2 | 0.8 | 868.2 | 151.2 | - | 74.0 |
| **3** | 5 | 1.5 | 0.6 | 348.3 | 26.47 | 3.136 | 10.6 |
| | 10 | 1.5 | 0.7 | 373.9 | 52.4 | 28.27 | 67.2 |
| | 20 | 1.3 | 0.6 | 327.9 | 132.3 | 33.88 | 84.1 |
| | 50 | 1.7 | 0.7 | 182.9 | 205.7 | 49.09 | 89.6 |

Nyquist diagrams for the synthesized carbohydrate derivatives are shown in figure 5. It can be observed a depressed semi-circle shape for all the compounds, which can be attributed to two-time

constants: one related to charge transfer resistance, and another one related to the adsorbed inhibitor film [21-23]. Compounds 5 and 6 showed charge transfer resistance dependence only [24].

Comparatively, Nyquist diagrams a, b and d, showed that, at 50 ppm, the diameter for the semi-circle is larger for compound **5** ($Z_{real}$~ 495 **Ω**cm$^2$). Structurally, compound **4** is a simple molecule which possess heteroatoms and in saturations capable of a better interaction with the metal surface, increasing the adsorption and improving corrosion inhibition in API 5L X70 steel. The protected -OH in compound **4** do not influences in the overall inhibition efficiency in concentrations over 20 ppm. Similarly, when the disubstituted compound (compound **5**) was tested, it showed a similar corrosion inhibition behavior for API 5L X70 steel under the studied conditions.

It is important to note that further modifying the structure of the carbohydrate does not increase the overall corrosion inhibition (compounds **7** and **8**) that the one showed by compound **4**.

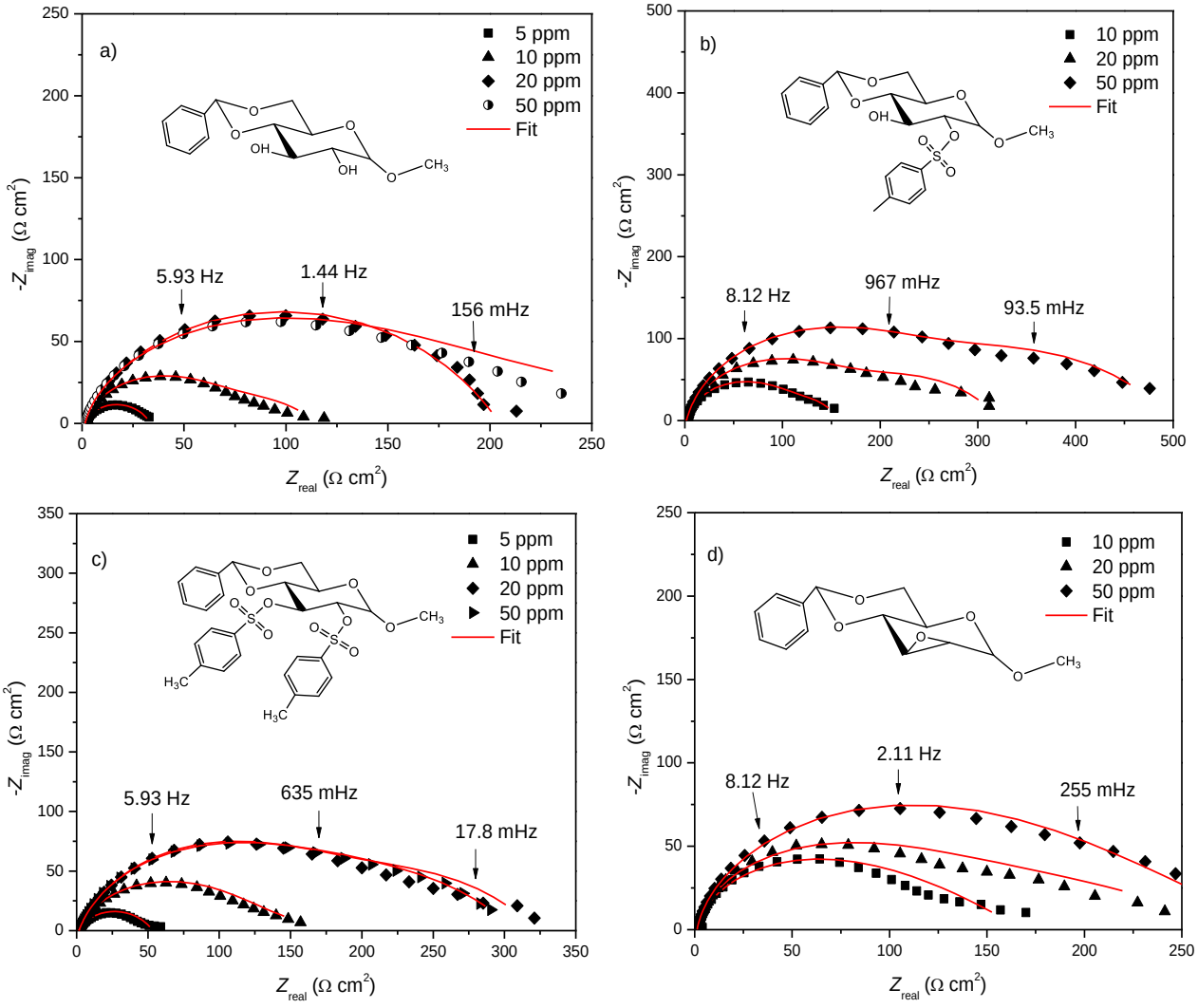

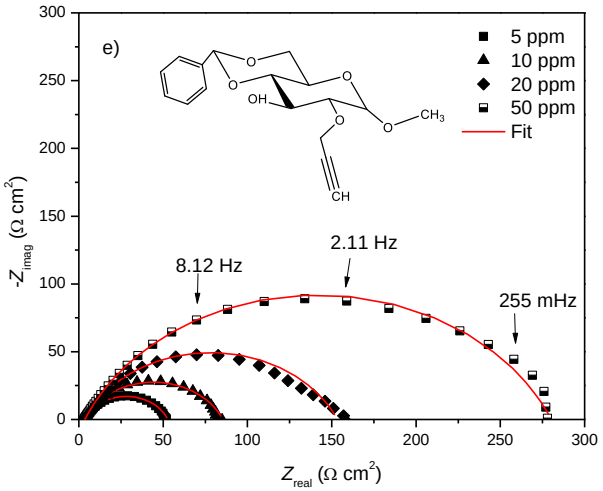


**Figure 5.** Nyquist diagrams of carbohydrate derivatives on immersed API 5L X70 steel at different inhibitor concentrations. Diagrams a), b), c), d) and e) corresponds to compounds 4, 5, 6, 7 and 8 respectively.

**Table 2.** Electrochemical parameters for carbohydrate derivatives in API 5L X70 steel immersed in HCl 1M

| **Compound** | ***C*** **(ppm)** | $R_s$ **(Ω cm²)** | **n** | $C_{dl}$ **(μFcm⁻²)** | $R_{ct}$ **(Ω cm²)** | $R_{mol}$ **(Ω cm²)** | $R_{total}$ **(Ω cm²)** | ***IE*** **(%)** |
|---|---|---|---|---|---|---|---|---|
| | **0** | 1.7 | 0.8 | 1927.2 | 40.2 | - | 40.2 | - |
| | **5** | 1.6 | 1.0 | 93.1 | 28.4 | 3.5 | 31.8 | - |
| 4 | **10** | 1.9 | 0.9 | 308.9 | 64.8 | 48.7 | 113.5 | 38.0 |
| | **20** | 2.0 | 1.0 | 87.3 | 199.1 | 3.8 | 202.9 | 79.8 |
| | **50** | 1.9 | 0.9 | 297.8 | 322.1 | 1.0 | 323.1 | 87.5 |
| | **5** | 1.6 | 0.9 | 2031.0 | 26.6 | 10.9 | 37.5 | - |
| | **10** | 1.5 | 0.9 | 326.3 | 113.0 | 42.8 | 155.8 | 64.5 |
| 5 | **20** | 1.5 | 0.9 | 358.0 | 173.3 | 146.9 | 320.2 | 76.8 |
| | **50** | 1.6 | 0.9 | 277.0 | 240.0 | 255.4 | 495.4 | 83.3 |
| | **5** | 1.6 | 1.0 | 1104.0 | 50.5 | 1.4 | 51.8 | 22.5 |
| | **10** | 2.0 | 0.8 | 107.5 | 175.2 | 0.0 | 175.2 | 77.1 |
| 6 | **20** | 2.1 | 0.8 | 418.8 | 184.3 | 134.6 | 318.9 | 78.2 |
| | **50** | 1.6 | 0.8 | 416.2 | 170.0 | 135.4 | 305.4 | 76.4 |
| | **5** | 3.9 | 0.7 | 355.1 | 34.2 | - | 34.2 | - |
| 7 | **10** | 1.7 | 1.0 | 104.8 | 165.9 | - | 165.9 | 75.8 |
| | **20** | 1.3 | 1.0 | 198.3 | 276.8 | - | 276.8 | 85.5 |
| | **50** | 1.2 | 0.9 | 250.0 | 294.8 | - | 294.8 | 86.4 |
| | **5** | 3.4 | 0.8 | 229.2 | 49.9 | - | 49.9 | 19.5 |
| 8 | **10** | 3.2 | 0.8 | 312.4 | 83.1 | - | 83.1 | 51.7 |
| | **20** | 3.2 | 0.7 | 343.2 | 150.1 | - | 150.1 | 73.2 |
| | **50** | 3.6 | 0.8 | 296.3 | 272.4 | 2.3 | 274.7 | 85.3 |

Figure 6 shows the corrosion inhibition as function of concentration of the carbohydrate. As can be seen, a lower corrosion of the metal (higher *IE*) correlates with a higher concentration of the carbohydrates. Lactose remains as the best corrosion inhibitor for concentrations above 20 ppm for the commercially available carbohydrates, while compound **4** showed the best corrosion inhibition

efficiency for the synthesized carbohydrate derivatives. This is an indicative that the sulfoxide moiety does not improve the efficiency of the carbohydrate as corrosion inhibitor. Moreover, it seems that the -OH substituents in the hexose ring are responsible for the corrosion inhibition and for the interaction of the carbohydrate with the metal surface and, derivatization of this substituents leads to a loss in efficiency as corrosion inhibitor.

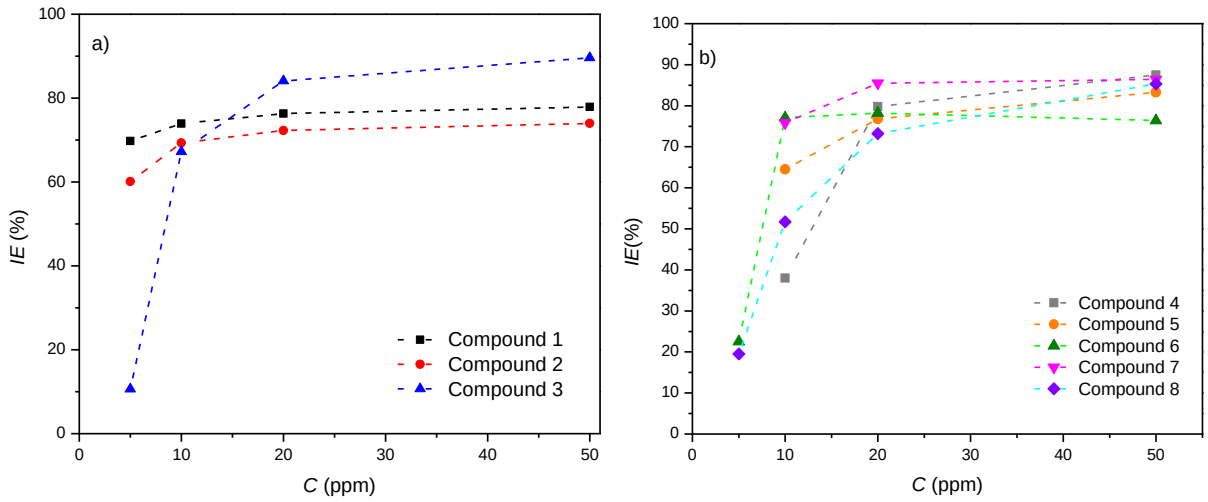


**Figure 6**. Variation of the inhibition efficiency of the carbohydrate derivatives 1-8 as a function of its concentration for API 5L X70 steel submerged in HCl 1M.

*3.2 Corrosion inhibition test by polarization curves for carbohydrates at 50 ppm for API 5L X70 steel in acid conditions.*

The electrochemical parameters obtained by potentiodymic polarization technique, using the Tafel extrapolation were: the corrosion potential ($E_{corr}$), the corrosion current density ($i_{corr}$) and both; the anodic and cathodic Tafel slopes ($b_c$ and $b_a$). The inhibition efficiency (*IE* %) values were determined using equation 4 [25] and are presented in Table 3.

$$IE(\%) = (1 - \frac{i\ \mathrm{corr}}{i\ \mathrm{corr(blank)}})\ \mathrm{x}\ 100 \quad (4)$$

Where, $i_{corr}$(blank) is a corrosion current density without inhibitor and $i_{corr}$ is the corrosion current density in the presence of carbohydrate inhibitor

In Table 3 it can be observed that $i_{corr}$ decreased in the presence of 50 ppm carbohydrate inhibitors, indicating that the anodic dissolution of carbon steel and cathodic reduction of hydrogen ions were inhibited; this suggests the formation of a protective layer of inhibitor molecules over the steel surface [26]. However, cathodic reactions are comparatively more affected than the anodic ones without causing any significant change in $E_{corr}$ values (< 85 mV) which leads us to conclude that carbohydrates are a mixed type but predominantly it is a cathodic type inhibitor (see Figure 7) [27].

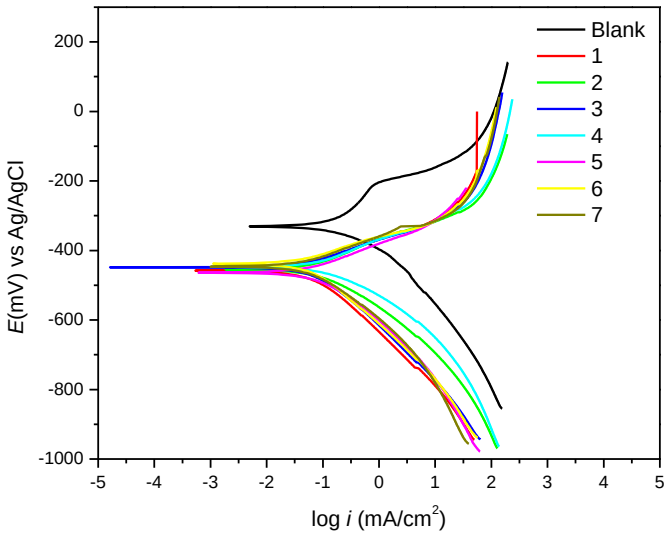


**Figure 7.** Tafel plots in the absence and presence at 50 ppm of carbohydrate derivatives 1-8 for API 5L X70 steel submerged in HCl 1M

**Table 3.** Polarization data in the absence and presence of 50 ppm carbohydrate derivatives 1-8 for API 5L X70 steel submerged in HCl 1M

| Compound | *C* (ppm) | $E_{corr}$ vs Ag/AgCl sat. | $-b_c$ (mV $dec^{-1}$) | $b_a$ (mV $dec^{-1}$) | $i_{corr}$ (μA/$cm^2$) | *Θ* | *IE* (%) |
|---|---|---|---|---|---|---|---|
| **Blank** | 0 | -331.0 | 173.4 | 125.1 | 530.3 | | |
| **1** | 50 | -458.6 | 149.1 | 70.8 | 66.0 | 0.9 | 87.6 |
| **2** | 50 | -455.2 | 121.3 | 76.5 | 126.9 | 0.8 | 76.1 |
| **3** | 50 | -447.0 | 145.2 | 62.2 | 69.2 | 0.9 | 86.9 |
| **4** | 50 | -445.4 | 118.3 | 79.2 | 208.1 | 0.6 | 60.8 |
| **5** | 50 | -463.2 | 139.1 | 77.8 | 98.5 | 0.8 | 81.4 |
| **6** | 50 | -441.5 | 135.7 | 57.7 | 56.5 | 0.9 | 89.3 |
| **7** | 50 | -445.1 | 130.4 | 65.3 | 67.9 | 0.9 | 87.2 |

*3.3 Adsorption isotherm*

Among all the adsorption mechanism descriptions reported in the literature [28-33], the most common model to describe this process is Langmuir's isotherms (equation 5). The corresponding adjustment for this model was performed and is shown in figure 8, while the adjustment parameters are shown in Table 3.

$$\frac{C}{\theta} = \frac{1}{k_{ads}} + C \quad (5)$$

Where *C* is the concentration, *Θ* is the coating degree and $k_{ads}$ is the adsorption constant.

The value of $k_{ads}$ is related with the Gibbs free energy value ($\Delta G°_{ads}$) and is related to equation (6) [34, 35]:

$$\Delta G°_{ads} = -RT\ ln\ 55.5 k_{ads} \quad (6)$$

Where the numeric value of 55.5 is the molar concentration of water in an acid solution, *R* is the constant of ideal gasses and *T* is the absolute temperature of the system.

The calculated values of the thermodynamic adjustment are also shown in Table 3. Several authors mention that the values of $\Delta G°$ ads around -40 KJ/mol or more negative are consistent with the charge interchange between the metal and the organic compound, so the reaction is defined as a chemisorption, while the values of $\Delta G°$ ads lower than -20 KJ/mol produce only an electrostatic interaction (physisorption) [36-41].

According to these results, for all the compounds a physisorption-chemisorption type process is observed, with exception to compound 6, which presents only a chemisorption type process [42].

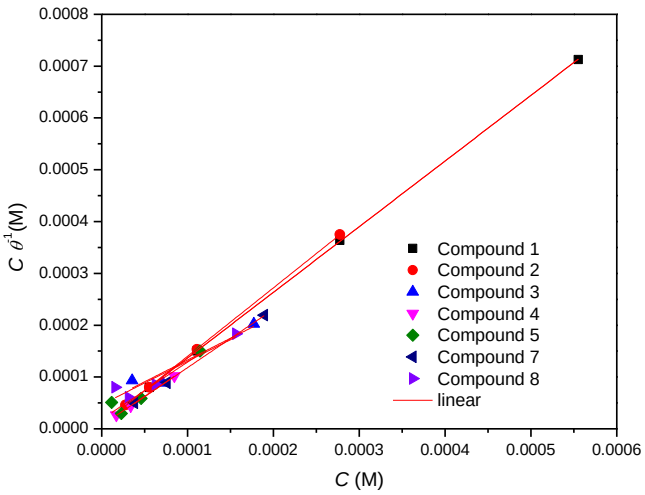


**Figure 8.** Adsorption isotherm at different concentrations of carbohydrates derivatives on API 5L X70 steel immersed in 1M HCl

**Table 3.** Adjustment of thermodynamic data with the Langmuir isotherm

| **Compound** | **$\Delta G°_{ads}$ (KJ/mol)** | **$R^2$** | **Compound** | **$\Delta G°_{ads}$ (KJ/mol)** | **$R^2$** |
|---|---|---|---|---|---|
| **1** | -36.84 | 1 | **5** | -38.71 | 0.9998 |
| **2** | -38.39 | 0.9999 | **6** | -43.43 | 0.9999 |
| **3** | -37.82 | 0.9988 | **7** | -39.09 | 0.9995 |
| **4** | -33.92 | 0.9252 | **8** | -33.92 | 0.9133 |

*3.4 SEM-EDS Surface analysis*

The surfaces of the API 5L X70 steel with and without inhibitor (Figure 9), were characterized by SEM-EDS to corroborate the effectiveness of the inhibitor by evaluating the electrochemical response. Figure 9a shows the surface of polished steel without the presence of inhibitor. As can be appreciated, the metallic surface presents damage due to the action of chloride ions in the corrosive solution, supported by EDS and shown in Figure 9b. However, figures 9c and 9e show the morphology of the steel sample surface in presence of the best carbohydrate inhibitors found in this research (compounds **3** and **7**). These results suggest that the inhibitors form protective films of the surface of the

API 5L X70 steel effectively diminishing corrosion. In this case, the corrosive species ($Cl^-$) are diminished in the chemical analysis (Figures 9d and 9f).

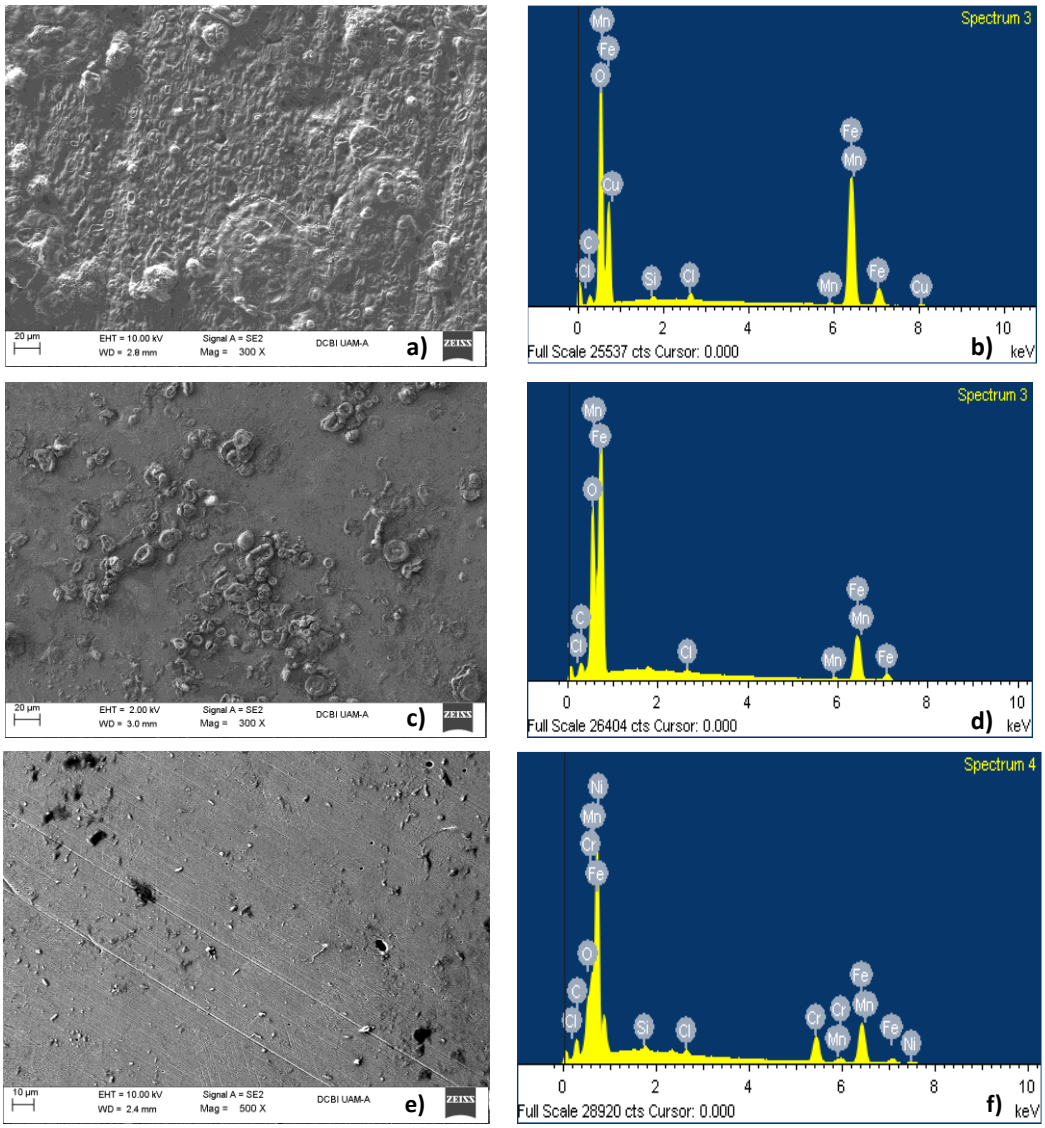


**Figure 9.** SEM-EDS images of API 5L X70 steel for a) polished steel immerse in HCl 1M, in presence of 50 ppm of c) compound 3 and e) compound 7.

## 4. CONCLUSIONS

Five of eight of the carbohydrates proved to be efficient corrosion inhibitors for API 5L X70 steel submerged in HCl 1M under static conditions. Lactose showed a better performance that glucose

and galactose under the studied conditions. However, the best corrosion inhibition efficiency was showed by Methoxy-4,6-O-Benzylidene-α-D-glucopyranose (Compound 4).

Thermodynamic analysis showed that all of the studied carbohydrates followed a combined physical-chemical adsorption process over the metal surface. This was correlated with the electron spectroscopy analysis of the metal surface.

ACKNOWLEDGEMENTS
Proyect No. 116061 Basic Science CONACyT. AEV thanks CONACyT posdoctoral fellow. Authors would like to thank Laboratorio Interdisciplinario de Electroquímica, Laboratorio de Corrosión y Protección de la Facultad de Química-UNAM and SNI. We thank The Divisional Electronic Mycroscopy Lab (Laboratorio Divisional de Microscopía Electrónica) for the use of Zeiss SUPRA 55 VP microscope.

## References

1. E.E. Ebenso, B. Huang, Y. Lin, W. Liu, J. Pan and A. Singh, *J. Ind. and Eng. Chem*., 24 (2015) 219.
2. A.K. Singh, S. Thakur, B. Pani and G. Singh, *New J. Chem*., 42 (2018) 2113.
3. G. Vengatesh, G. Karthik and M. Sundaravadivelu, *Egypt. J. Petrol.*, 26 (2017) 705.
4. F. Bentiss, B. Hammouti, T. Lakhlifi, M. Traisnel, H. Vezin and A. Zarrouk, *Corros. Sci*., 90 (2015) 572.
5. S. Deng, G. Du, X. Li and X. Xie, *Corros. Sci.*, 87 (2014) 27.
6. N.K. Gupta, P.G. Joshi, M.A. Quraishi and V. Srivastava, *Int. J. of Biol. Macrom*., 106 (2018) 704.
7. A. Espinoza, E. Hernández, H. Herrera, G. Fajardo, M.I. Franco and J.G. Miranda, *Av. Cien. Ing.*, 6(3) (2015) 9.
8. G.A. Pasquale, G.P. Romanello, D.M. Ruiz, Química de la Biomasa y los Biocombustibles, 1ª Ed. Editorial de la Universidad de la Plata, (2016) Boyaca, Colombia.
9. J. Caballero, M.A. Martínez, S. Rebollar, B. Rendon, Estudio sobre la relación entre seres humanos y plantas en los albores del siglo XXI, (2001) Iztapalapa, México.
10. H.M. Barbosa, A. Espinoza and F.J. Rodríguez, *MRS Adv*., 2 (2017) 3909.
11. K. Haruna, I.B. Obot, N.K. Ankah, A.A. Sorour and T.A. Saleh, *J. Mol. Liq.* 264 (2018) 515.
12. G. Liua, M. Xue and H. Yang, *Desalination*, 419 (2017) 133.
13. Y. Qiang, S. Zhang, S. Yan, X. Zou and S. Chen, *Corros. Sci*., 126 (2017) 295.
14. A.A. Khadom, A.N. Abd and N.A. Ahmed, *S. Afr. J. Chem. Eng*., 25 (2018) 13.
15. A.A. Al-Amierya, M.H. Othman, T. Adnan, T. Sumer and A. Amir, *Results Phys*., 9 (2018) 978.
16. R. Haldhar, D. Prasad and A. Saxena, *J. Environ. Chem. Eng*., 6 (2018) 5230.
17. D. Singh, K.R. Ansari, A.A. Sorour, M.A. Quraishi, H. Lgaz and R. Salghi, *Int. J. Biol. Macromol*., 107 (2018) 1747.
18. M. Mobin, M. Basik and J. Aslam, *J. Mol. Liq.*, 263 (2018) 174.
19. M. Messali, M. Larouj, H. Lgaz, N. Rezki, F.F. Al-Blewi, M.R. Aouad, A. Chaouiki, R. Salghi and I. Chung, *J. Mol. Struct*., 1168 (2018) 39.
20. C. Verma, J. Haque, E.E. Ebenso and M.A. Quraishi, *Results Phys*., 9 (2018) 100.
21. J. Haquea, C. Verma, V. Srivastava, M.A. Quraishi and E. E. Ebenso, *Results Phys*., 9 (2018) 1481.
22. A.S. Fouda, M.A. Ismail, G.Y. EL-ewady and A.S. Abousalem, *J. Mol. Liq.*, 240 (2017) 372
23. P. Dohare, K.R. Ansari, M.A. Quraishi and I.B. Obot, *J. Ind. and Eng. Chem.*, 52 (2017) 197.
24. F. El-Hajjaji, M. Messali, A. Aljuhani, M.R. Aouad, B. Hammouti, M.E. Belghiti, D.S. Chauhan and M.A. Quraishi, *J. Mol. Liq.*, 249 (2018) 997.
25. H.J. Habeeb, H.M. Luaibi, T.A. Abdullah, R.M. Dakhil, A.A.H. Kadhuma and A.A. Al-Amierye, *Case Studies in Thermal Engineering*, 12 (2018) 64.

26. T. Rabizadeh and S. Khameneh Asl, *J. Mol. Liq.,* 276 (2019) 694.
27. P.E. Álvarez, M.V. Fiori-Bimbi, A. Neske, S.A. Brandán and C.A. Gervasi, *J. Ind. Eng. Chem*., 58 (2018) 92.
28. R.K. Gupta, M. Malviya, C. Verma and M.A. Quraishi, *Mater. Chem. Phys*., 198 (2017) 360.
29. E.A. Badra, M.A. Bedair and S. M. Shabana, *Mater. Chem. Phys*., 219 (2018) 444.
30. V. Srivastava, J. Haque, C. Verma, P. Singh, H. Lgaz, R. Salghi and M.A. Quraishi, *J. Mol. Liq.,* 244 (2017) 340.
31. D.K. Singh, E.E. Ebenso, M.K. Singh, D. Behera, G. Udayabhanu and R.P. John, *J. Mol. Liq*. 250 (2018) 88.
32. H. Hamania, T. Douadia, D. Daouda, M. Al-Noaimic, R.A. Rikkouha and S. Chafaaa, *J. Electroanal. Chem*., 801 (2017) 425.
33. X. Ma, X. Jiang, S. Xia, M. Shan, X. Li, L. Yu and Q. TangbaKey, *Appl. Surf. Sci*., 371 (2016) 248.
34. R. Haldhar, D. Prasad and A. Saxena, *J. Environ. Chem. Eng.,* 6 (2018) 2290.
35. Q. Maa, S. Qia, X. Hea, Y. Tang and G. Lub, *Corros. Sci*., 129 (2017) 91.
36. P. Singh and M.A. Quraishi, *Measurement*, 86 (2016) 114.
37. M. Farsak, H. Keles and M. Keles, *Corros. Sci.*, 98 (2015), 223.
38. Z. Hu, Y. Meng, X. Ma, H. Zhu, J. Li, C. Li and D. Cao, *Corros. Sci.*, 112 (2016) 563.
39. A.H. El-Askalany, S.I. Mostafa, K. Shalabi, A.M. Eida and S. Shaabana, *J. Mol. Liq*., 223 (2016) 497.
40. W. Gayed and N.H. El-Sayed, *Europ. J. of Chem*., 5 (2014) 563.
41. R. Yıldız, *Corros. Sci.,* 90 (2015) 544.
42. P. Mohan and G. Paruthimal, *J. Mater. Sci. Techno.*, 29 (2013) 1096.